Planet. Space Sci., Vol. 38, No. 10, pp. 1243–1250, 1990
Printed in Great Britain.

0032–0633/90 $3.00+0.00
Pergamon Press plc

COMPARISON OF A LOW-LATITUDE IONOSPHERIC MODEL WITH OBSERVATIONS OF OI 630 nm EMISSION AND IONOSPHERIC PARAMETERS

Y. SAHAI, J. A. BITTENCOURT and H. TAKAHASHI
Instituto de Pesquisas Espaciais-INPE, C. P. 515, 12201 São José dos Campos, SP, Brasil

and

M. MENDILLO

Center for Space Physics, Boston University, Boston, MA 02215, U.S.A.

(*Received in final form* 16 *May* 1990)

Abstract—A comparative study is carried out between a semi-empirical low-latitude ionospheric model (SLIM), including calculated OI 630 nm airglow emission intensities predicted by the SLIM model, with ionospheric and OI 630 nm airglow measurements carried out at Cachoeira Paulista (22.7°S, 45.0°W; geomag. 11.9°S), Brazil. A long series of regular measurements of ionospheric *F*-region peak electron densities and peak heights, and regular zenith measurements of the OI 630 nm airglow emission intensities, made during the period 1975–1982, are used for comparison with corresponding parameters predicted by the SLIM model. Large discrepancies between the observed and model-predicted OI 630 nm intensities have been found for high solar activity, mainly due to an overestimate of the *F*-region peak heights by the SLIM model. Use of SLIM profiles normalized by actual *F*-region peak height and density observations essentially removed the disagreements. The reasons for the height discrepancies are discussed in terms of the longitudinal dependence of the geomagnetic control on the $\mathbf{E} \times \mathbf{B}$ vertical plasma drifts and the thermospheric neutral wind effects on the *F*-region. The effects of the magnetic declination angle on both the $\mathbf{E} \times \mathbf{B}$ ionospheric plasma drifts and thermospheric neutral winds at low-latitude suggest that ionospheric models need to address separately the longitudinal zones of magnetic declination either positive, negative or zero.

INTRODUCTION

During recent years various empirical ionospheric models have been developed (see e.g. Llewellyn and Bent, 1973; Chiu, 1975; Rawer, 1981) for predicting ionospheric parameters for radio communication applications. These ionospheric models can be used for comparative studies of observed ionospheric properties with model predictions for different geophysical and solar activity conditions. In conjunction with suitable neutral atmospheric models, the ionospheric models permit stimulating the behaviour of OI 630 nm nightglow emission intensity. This emission is an optical indicator of several ionospheric processes in the upper atmosphere (Serafimov *et al.*, 1977) and has been used to study *F*-region peak height variations (Tinsley and Bittencourt, 1975; Chandra *et al.*, 1975; Sahai *et al.*, 1981b), thermospheric neutral winds (Bittencourt and Tinsley, 1976, 1977; Bittencourt *et al.*, 1976) and *F*-region plasma irregularities (Weber *et al.*, 1978; Sahai *et al.*, 1981a; Sobral *et al.*, 1981; Mendillo and Baumgardner, 1982).

Anderson *et al.* (1985, 1987) have described a semi-empirical low-latitude ionospheric model (SLIM) and presented theoretically calculated electron density profiles, OI 630 nm airglow intensities and total electron content (TEC), as a function of latitude (between 24°N and 24°S dip latitude). A fully analytical version of the SLIM model, emphasizing the behaviour of the low-latitude ionospheric *F*-region for various seasonal and solar cycle conditions, has been recently described by Anderson *et al.* (1989), referred to as the FAIM model. These models are based on the solution of the time-dependent continuity equation considering only the dominant O^+ ions and taking into account $\mathbf{E} \times \mathbf{B}$ drifts and thermospheric neutral winds. Anderson *et al.* (1987) have compared the OI 630 airglow intensities calculated using the SLIM model with the iso-intensity contours of the OI 630 nm airglow observations (autumn, solar maximum) conducted by the *AE-E* satellite (Abreu *et al.*, 1982) and have obtained a reasonable agreement only in the early part (up to about 21:00 L.T.) of the night. Fesen and Abreu (1987) have presented a comparative study of the observations of the OI 630 nm nightglow from *AE-E* (spring, solar maximum) and a theoretical model, and have suggested that tidal effects are important to reproduce the observed airglow intensities.

Regular zenith intensity measurements of the OI 630 nm nightglow emission have been carried out at Cachoeira Paulista (22.7°S, 45.0°W; geomag. 11.9°S), Brazil, since 1975. In this communication we present a comparative study of the OI 630 nm emission intensities observed at Cachoeira Paulista from 1975 to 1982 with the SLIM calculated airglow intensities for different seasons (equinox, winter and summer) under both solar maximum and solar minimum conditions at 12°S dip latitude (Anderson *et al.*, 1985). For solar maximum conditions, comparisons between the *F*-region peak electron densities and layer heights observed from the ionosonde at Cachoeira Paulista and the SLIM calculated *F*-region parameters for 12°S dip latitude (Anderson *et al.*, 1985) are also presented. The ionosonde data coverage for solar minimum conditions, corresponding to the airglow data used in this study, are insufficient for comparison and, therefore, are not presented here.

DATA BASE

Observations of the OI 630 nm nightglow emission have been carried out at Cachoeira Paulista on a routine basis since 1975. Measurements taken between March 1975 and June 1980 were carried out with a two-channel tilting filter photometer with a field of view of 5° full angle. The interference filter used had an effective diameter of 2 in. and bandwidth of 1.1 nm. An uncooled EMI-9558 photomultiplier was used and analog signals were recorded on a Kipp and Zonen micrograph recorder. A six-channel tilting filter photometer with a field of view of 3° full angle replaced the earlier photometer for the OI 630 nm emission observations in July 1980. The interference filter used has a 2 in. diameter with 1.0 nm bandwidth. A cooled EMI-9659B photomultiplier has been used in the photon-counting mode. A radioactive (Kr85) light source (American Atomic Corporation, U.S.A.) has been used for calibration of the photometers. The source was calibrated at Fritz Peak Observatory, NOAA, Boulder, U.S.A., in 1971 and recalibrated with our calibrated Eppley lamp in 1982. Absolute intensities were calculated using tilting filter (Yano, 1966) and calibration (Kulkarni and Sanders, 1964) techniques. The OH contamination has been considered negligible as narrow band filters have been used. The absolute calibration is estimated to have an accuracy of $\pm 10\%$. Data used in the present analysis included only those nights for which observations for more than 5 h were available.

The OI 630 nm observations obtained from March 1975 to February 1977 and from March 1979 to February 1981 have been used for solar minimum and maximum conditions, respectively. The ionospheric data presented for solar maximum conditions were obtained from an ionosonde operating on a routine basis at Cachoeira Paulista. The ionograms obtained during the months of December 1980, March–April 1981 and July 1981 have been considered as representative of solar maximum summer, equinox and winter seasons, respectively. During the low solar activity period (1975–1976), there were many interruptions in the ionosonde measurements at Cachoeira Paulista.

RESULTS

The OI 630 nm emission at low latitudes results mainly from dissociative recombination of O_2^+ ions (e.g. Peterson and Van Zandt, 1969). Using the same formalism and notation as that of Tinsley and Bittencourt (1975), the column emission rate, I_{630}, can be written as

$$I_{630} = KA_{630}n_m(e)\int \frac{\gamma_1 n(O_2)S(z)dz}{A[A+d(z)/A][1+B(z)]}. \tag{1}$$

This emission intensity is known to be strongly dependent on the *F*-region peak height, with a much smaller dependence on the peak electron density $n_m(e)$, since it involves the column integral of the product $n(O_2)$ $S(z)$, where $n(O_2)$ is the molecular oxygen density and $S(z)$ is a shape function for the *F*-region electron density. At low latitudes, the variations in the *F*-region height and the morphology of the equatorial ionospheric anomaly are governed primarily by the $\mathbf{E}\times\mathbf{B}$ vertical plasma drifts, but are also influenced by the thermospheric neutral winds.

In Fig. 1, we present the observed nocturnal mean intensity variations of the OI 630 nm nightglow emission for winter (May, June, July and August), summer (November, December, January and February) and equinox (March, April, September and October) for both solar cycle maximum (March 1979–February 1981) and minimum (March 1975–February 1977) conditions. The number of nights for which data were available in the different seasons to calculate the average intensities at each half-hour are indicated in parentheses. In the same figure we also present, for comparison purposes, the OI 630 nm emission intensities calculated using the SLIM model for 12°S dip latitude (Anderson *et al.*, 1985) for the different seasons under both solar maximum and minimum conditions.

It is evident from Fig. 1 that for solar cycle minimum conditions the observed and calculated intensity

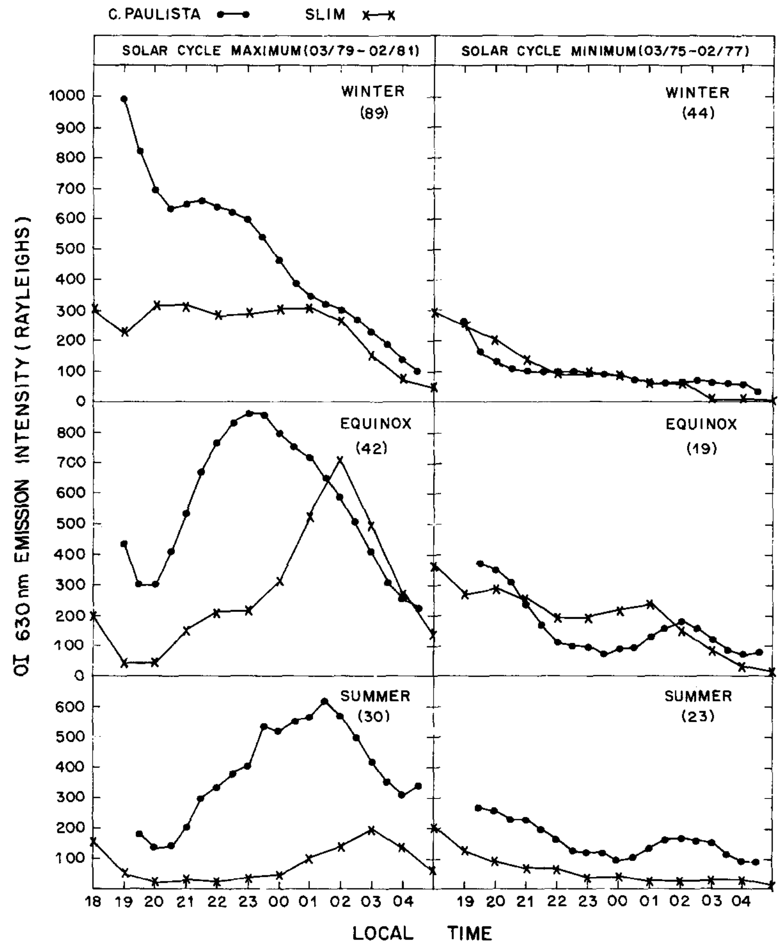

FIG. 1. MEAN NOCTURNAL INTENSITY VARIATIONS OF THE OI 630 nm EMISSION (DOTS) OBSERVED AT CACHOEIRA PAULISTA, BRAZIL, FOR DIFFERENT SEASONS DURING SOLAR MAXIMUM (1979–1981) AND MINIMUM (1975–1977) CONDITIONS.
The calculated OI 630 nm emission using the SLIM model for 12°S dip latitude are shown by crosses.

variations with local time are rather similar. However, for solar maximum conditions, the observed intensities are generally much larger than the calculated ones, except during the later part of the night (after ~01:00 L.T.) for winter and equinox. Also, the local time of the observed maximum intensities (winter ~21:30 L.T.; equinox ~23:00 L.T.; summer ~01:30 L.T.) differ significantly from the calculated intensity maximum local times (winter—no significant peak; equinox ~02:00 L.T.; summer ~03:00 L.T.).

In order to investigate the reasons for these large discrepancies in the nocturnal intensity variations during solar cycle maximum conditions, a comparative study has been made between observed and calculated ionospheric *F*-region parameters. In Figs 2–4, we present the local time variations of the mean *F*-region peak electron densities $n_m(e)$ and mean peak heights (h_pF2) obtained from ionograms taken at Cachoeira Paulista, with the corresponding variations calculated using the SLIM model for 12°S dip latitude for the different seasons (Anderson *et al.*, 1985). The numbers shown in parentheses indicate the number of days for which ionospheric data were available to calculate the mean *F*-region parameters at each hour during the different seasons.

The observed and model-predicted *F*-region peak electron density local time variations are quite similar. However, the observed *F*-region peak electron densities are smaller than the ones predicted by the SLIM model in the period from about 11:00 L.T. to 02:20

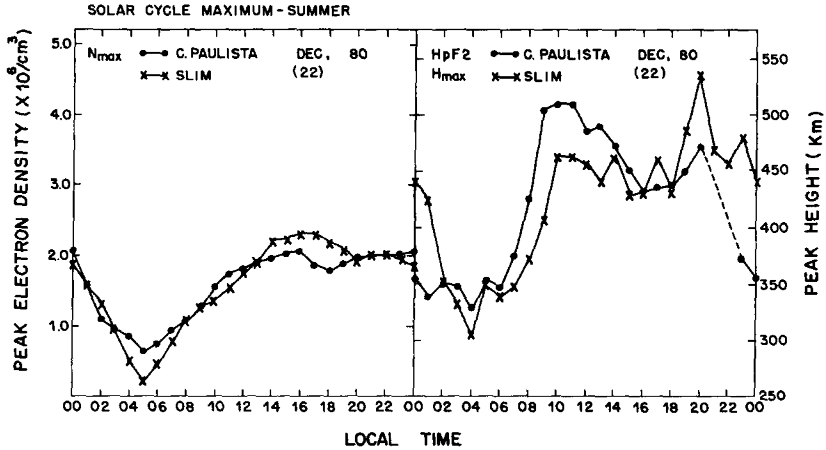

FIG. 2. MEAN DAILY VARIATIONS OF THE F-REGION PEAK ELECTRON DENSITIES AND PEAK HEIGHTS (DOTS) OBSERVED AT CACHOEIRA PAULISTA, BRAZIL, FOR SUMMER AND SOLAR MAXIMUM CONDITIONS.
The F-region peak electron densities and peak heights for 12°S dip latitude, calculated using the SLIM model for summer and solar maximum conditions, are shown by crosses.

L.T., except for the summer season where the agreement is fairly good. Also, the behaviour of the F-region peak height local time variations shows a somewhat similar trend. However, the model-predicted F-region peak heights are much higher than the observed ones in the afternoon period (except in summer), and this difference is much more pronounced in the evening and early part of the night.

Since the OI 630 nm emission is strongly height dependent, the large differences between the observed and the model-predicted F-region peak heights (Figs 2–4) will result in model-predicted OI 630 nm intensities much lower than the observed ones. The comparison between SLIM-generated electron density profiles and the empirical models of Chiu (1975) and Llewellyn and Bent (1973), shown in Figs 5 and 6 of Anderson et al. (1987), also indicates that the SLIM-generated F-region peak heights are much higher than those predicted by other models.

In order to investigate further the reasons for the differences between the model-predicted and observed OI 630 nm emission intensities and ionospheric parameters, we calculated the OI 630 nm column integrated intensities for each hour of the different seasons

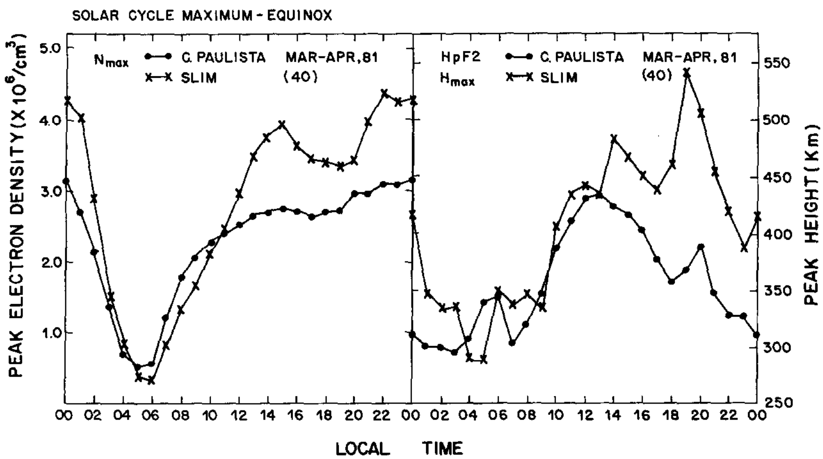

FIG. 3. SAME AS IN FIG. 2, BUT FOR EQUINOX CONDITIONS.

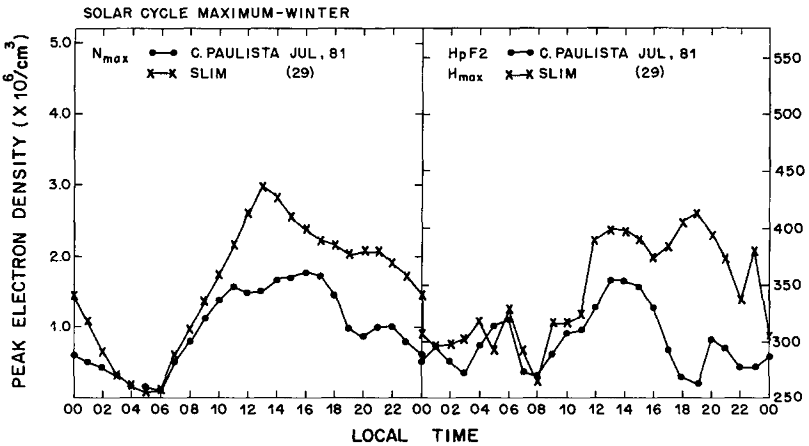

FIG. 4. SAME AS IN FIG. 2, BUT FOR WINTER CONDITIONS.

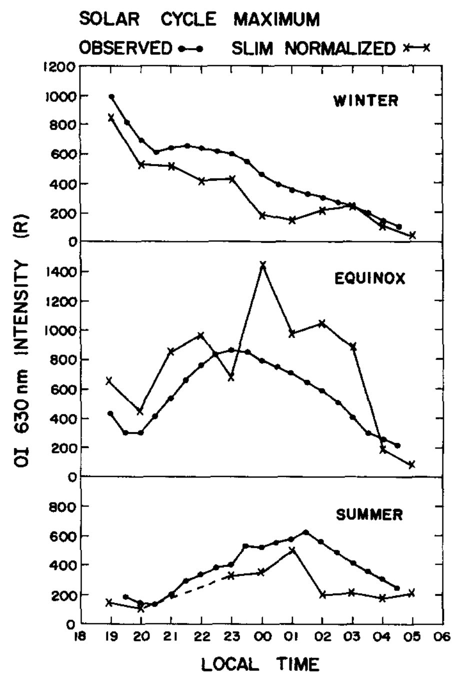

FIG. 5. COMPARISON OF THE OBSERVED MEAN NOCTURNAL INTENSITY VARIATIONS OF THE OI 630 nm EMISSION WITH AIRGLOW PRODUCTION COMPUTED FROM NORMALIZED SLIM PROFILES FOR DIFFERENT SEASONS.

using SLIM-generated electron density profiles for 12°S that were normalized to the observed ionospheric parameters (f_oF2 and h_pF2) at Cachoeira Paulista. For these calculations, we used the MSIS-86 neutral atmospheric model (Hedin, 1987) and the rate coefficients as given in Sahai *et al.* (1981b). Comparisons of the observed OI 630 nm intensities with airglow production computed from the normalized SLIM electron density profiles, as indicated above, are shown in Fig. 5, for the different seasons during solar cycle maximum conditions. The absence of calculated intensities as 21:00 and 22:00 L.T. during the summer season (December, 1980) is due to occurrence of spread-*F* at these hours on most of the nights of ionospheric measurements used in the present study.

In general, the local time variations of the observed and calculated intensities of the OI 630 nm emission show similar patterns and fairly good agreement. It must be pointed out that the observed average airglow pattern encompassed data spread over several months during a given season, while the ionospheric parameters used to normalize the SLIM electron density profiles, and employed to calculate the airglow intensities, are hourly averages restricted to December 1980 (summer), March–April 1981 (equinox) and July 1981 (winter). The discrepancies between the observed and calculated intensities during the hours near midnight are due to variations in the shape of the SLIM-generated electron density profiles, particularly in the bottomside of the *F*-layer. In Fig. 6, we present, for illustration, the SLIM-generated electron density profiles, normalized to the observed peak electron densities and peak heights for 22:00–24:00 L.T. during equinox. It can be seen that even though the observed peak electron densities and peak heights are the same at 22:00 and 23:00 L.T. (Fig. 3), the calculated intensities using the normalized SLIM profiles are different (Fig. 5), due to the difference in the shape of the layer profile, particularly in the bottomside, where the effects are significant in the OI 630 nm emission intensities. As discussed in the following section, these

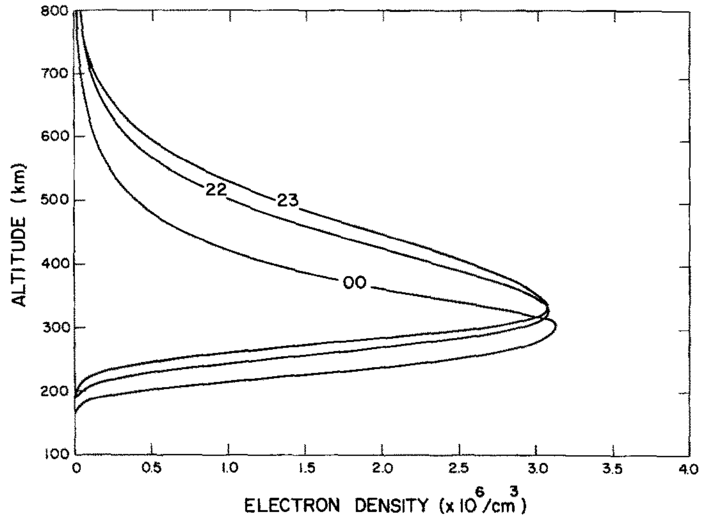

Fig. 6. Normalized SLIM-generated electron density profiles for 22:00, 23:00 and 00:00 L.T. during equinox.

variations in the shape of the SLIM-generated electron density profiles seem to be a consequence of the dynamical components used in the SLIM model. The theoretical, computer-generated electron density profiles that form the basis of SLIM result from coupled dependences of local time, **E** × **B** drifts and neutral winds. Therefore, just normalizing the SLIM-generated profiles to the observed electron density and peak height, without correspondingly adjusting the *shape* of the layer, may not be strictly adequate.

Summarizing, the comparisons presented in this study indicate that, in general, the SLIM model provides adequate results for solar minimum conditions. For high solar flux conditions, however, SLIM gives *F*-region peak heights that are higher and peak electron densities larger (except in summer) than the observed ones. An attempt to use the SLIM-generated electron density profiles normalized to the observed ionospheric parameters to calculate the OI 630 nm emission intensities did result in a much better agreement between the local time variations of the observed and calculated OI 630 nm emission intensities. Some residual discrepancies, particularly near midnight hours, are probably due to inadequate layer shape variations during these hours.

DISCUSSION

The present observational results (Figs 1–4), based on airglow and ionospheric measurements made in the Brazilian longitudinal sector, suggest that the assumed **E** × **B** vertical plasma drift models used in the SLIM-generated electron density profiles, which are based on Jicamarca (12°S, 77°W), Perú, measurements (Woodman, 1970; Fejer *et al.*, 1979), and also the thermospheric neutral wind models, are possibly not appropriate for different longitudes.

The **E** × **B** vertical plasma drift velocity and its seasonal variations are known to be dependent on the magnetic declination angle at a given longitude as well as on the season (Abdu *et al.*, 1981; Batista *et al.*, 1986). Batista *et al.* (1986) have shown through an analysis of ionospheric data obtained at equatorial stations in Jicamarca and Huancayo (12°S, 75°W), Perú, and Fortaleza (3°S, 38°W), Brazil, the existence of significant seasonal and longitudinal differences in the behaviour of the **E** × **B** vertical plasma drifts. The nocturnal variations of the *F*-layer peak heights are greatly dependent on the amplitude and duration of the pre-reversal peak in the ionospheric *F*-region plasma vertical drifts. The pre-reversal peak is controlled by the sharp longitudinal gradients in the *E*-region integrated Pederson conductivity near sunset, as a result of the seasonal dependence of the angle between the geomagnetic meridian and the terminator (see also Tsunoda, 1985). Consequently, the magnetic declination angle at a given longitude has a great influence on the ionospheric vertical plasma drifts and their seasonal variations.

The SLIM model used the MSIS-83 (Hedin, 1983) neutral atmospheric model to calculate N_2, O_2, and O densities and the neutral temperature, considering average geomagnetic conditions with $A_p = 15$ and $F_{10.7}$ cm flux of 180 units to represent solar maximum conditions. In Table 1, we present the average $F_{10.7}$ cm fluxes and A_p with their standard deviations (σ) for the nights of the OI 630.0 nm observations during different seasons used in this study. It may be noted that the average values of $F_{10.7}$ cm flux and A_p for different seasons are fairly close to those used in the SLIM model. The main effect due to differences in the neutral densities and temperature would be to modify the day-to-day absolute intensity levels. Therefore, it seems that uncertainties in neutral density would not introduce significant differences in the nocturnal variations between the model and observational results.

In a recent paper Fejer *et al.* (1989) have presented and discussed measurements of equatorial *F*-region $\mathbf{E} \times \mathbf{B}$ ionospheric plasma drifts during solar maximum conditions at Jicamarca. They found that the ionospheric vertical plasma drifts are highly dependent on solar flux and magnetic activity. The effects of both solar flux and magnetic activity are different during equinoxes and solstices. It is also well known that the local time variations of the night-time *F*-region peak electron density and height, and of the OI 630.0 nm emission in the tropical region are strongly dependent on the local time behaviour of the $\mathbf{E} \times \mathbf{B}$ ionospheric plasma drifts, especially around sunset time (Bittencourt and Sahai, 1979). As pointed out earlier, the average values of A_p and $F_{10.7}$ cm flux for the observations are very similar to the ones used in the SLIM model. It seems, therefore, that the large differences between the observed and SLIM calculated OI 630.0 nm nocturnal variations could not be attributed to differences in the $\mathbf{E} \times \mathbf{B}$ ionospheric plasma drifts as a result of solar flux and magnetic activity effects.

The influence of the thermospheric neutral winds on the *F*-region height variations is also longitudinal dependent, since the velocity component along the field line depends on the local magnetic declination angle and on the relative latitudinal positions of the geographic and geomagnetic equators, as discussed by Bittencourt and Sahai (1978). The horizontal neutral wind velocity component along the magnetic meridian (u_θ) can be written as

$$u_\theta = u'_\theta \cos(\delta_m) + u'_\phi \sin(\delta_m), \qquad (2)$$

where, u'_θ denotes the geographical meridional component, u'_ϕ the geographical zonal component of the horizontal neutral wind velocity and δ_m is the magnetic declination angle. For example, a strong geographical zonal wind component (u'_ϕ) blowing from West to East during the night-time would produce opposite ionospheric effects in longitudinal sectors where magnetic declination angles are eastward or westward. Therefore, in view of the longitudinal differences in the magnetic field line morphology at low latitudes, it seems that appropriate $\mathbf{E} \times \mathbf{B}$ vertical plasma drifts and thermospheric neutral winds must be considered for different longitudes in order to develop a more realistic low-latitude ionospheric model. As a first step in creating a fully global low-latitude ionospheric model, it is suggested that separate regional models should be developed for longitudinal sectors with magnetic declination positive (American sector: 150°E–60°W), negative (Atlantic sector: 60°W–0°E) and zero (Indian sector; 0°–150°E) (Bittencourt *et al.*, 1976).

Table 1. Average $F_{10.7}$ cm fluxes and A_p

	Season	$\bar{A}_p$	σ	$\bar{F}_{10.7}$	σ
Present observations	Equinox	13.8	10.7	199.4	26.3
	Winter	12.0	7.2	172.2	37.0
	Summer	12.9	9.0	207.8	36.3
SLIM	All seasons	15.0	—	180	—

SUMMARY AND CONCLUSIONS

A comparative study between the low-latitude OI 630 nm emission intensities observed at Cachoeira Paulista and those predicted by the SLIM model (Anderson *et al.*, 1985, 1987) has been carried out for different seasons under both low and high solar activities. For the solar minimum comparisons, the SLIM predictions and the observational results showed an acceptable level of agreement. However, large discrepancies between the observed and model-predicted OI 630 nm intensities have been found for high solar activity. Detailed comparisons between the observed ionospheric parameters at Cachoeira Paulista and those predicted by the SLIM model for high solar activity showed that these discrepancies were due mainly to an overestimate of the *F*-region peak heights by the SLIM model, as the OI 630 nm intensity is strongly *F*-region height dependent. The *F*-region peak height variations are governed primarily by the $\mathbf{E} \times \mathbf{B}$ vertical plasma drifts and also by the thermospheric neutral winds. Their effects on the *F*-region peak heights are longitudinal dependent due to the longitudinal differences in geomagnetic field morphology at low latitudes. It is suggested that for different longitudinal regions where the magnetic declination angle is either positive, negative or zero, appropriate $\mathbf{E} \times \mathbf{B}$ vertical plasma drift and thermospheric wind models are necessary for a more realistic modelling of the low-latitude ionosphere and airglow.

Acknowledgements—Thanks are due to B. R. Clemesha for helpful discussions and comments. Thanks are also due to E. R. de Paula and I. S. Batista for providing the ionospheric data. P. Litis and R. Doe assisted in the SLIM-normalization analysis at Boston University. This work was partially supported by Fundo Nacional de Desenvolvimento Científico e Tecnológico (FNDCT), under contract FINEP-537/CT, by Conselho Nacional de Desenvolvimento Cientifico e Tecnológico (CNPq) through grant No. 400.273/86-FA, and by contract AFGL F19628-86-K-0026 to Boston University.

REFERENCES

Abdu, M. A., Bittencourt, J. A. and Batista, I. S. (1981) Magnetic declination control of the equatorial *F*-region dynamo electric field development and spread *F*. *J. geophys. Res.* **86**, 11443.

Abreu, V. J., Schmitt, G. A., Hays, P. B. and Dachev, T. P. (1982) Volume emission rate profiles of the 6300-Å tropical nightglow obtained from the *AE-E* satellite: latitudinal and seasonal variations. *J. geophys. Res.* **87**, 6346.

Anderson, D. N., Forbes, J. M. and Codrescu, M. (1989) A fully analytic low- and middle-latitude ionospheric model. *J. geophys. Res.* **94**, 1520.

Anderson, D. N., Mendillo, M. and Herniter, B. (1985) A semiempirical low-latitude ionospheric model. AFGL Tech. Rep. RT-85-0254, Air Force Geophys. Lab., Hanscom Air Force Base, MA.

Anderson, D. N., Mendillo, M. and Herniter, B. (1987) A semiempirical low-latitude ionospheric model. *Radio Sci.* **22**, 292.

Batista, I. S., Abdu, M. A. and Bittencourt, J. A. (1988) Equatorial *F*-region vertical plasma drifts: seasonal and longitudinal asymmetries in the American sector. *J. geophys. Res.* **91**, 12055.

Bittencourt, J. A. and Sahai, Y. (1978) *F*-region neutral winds from ionosonde measurements of *hmF*2 at low latitude magnetic conjugate region. *J. atmos. terr. Phys.* **40**, 660.

Bittencourt, J. A. and Sahai, Y. (1979) Behaviour of the OI 6300 Å emission at the magnetic equator and its relation to the vertical $\mathbf{E} \times \mathbf{B}$ plasma drift velocity. *J. atmos. terr. Phys.* **41**, 1233.

Bittencourt, J. A. and Tinsley, B. A. (1976) Tropical *F*-region winds from OI 1356-Å and OI 6300-Å emissions, 1. Theory. *J. geophys. Res.* **81**, 3781.

Bittencourt, J. A. and Tinsley, B. A. (1977) Nighttime thermospheric winds at low latitudes deducted from *AE-C* ionospheric measurements. *J. geophys. Res.* **82**, 4694.

Bittencourt, J. A., Tinsley, B. A., Hicks, G. T. and Reed, E. I. (1976) Tropical *F*-region winds from OI 1356-Å and OI 6300-Å emission, 2. Analysis of *OGO* 4 data. *J. geophys. Res.* **81**, 3786.

Chandra, S., Reed, E. I., Merier, R. R., Opal, C. B. and Hicks, G. T. (1975) Remote sensing of the ionospheric *F* layer using airglow techniques. *J. geophys. Res.* **80**, 2327.

Chiu, Y. T. (1975) An improved phenomenological model of ionospheric density. *J. atmos. terr. Phys.* **37**, 1563.

Fejer, B. G., Farley, D. T., Woodman, R. R. and Calderon, C. (1979) Dependence of equatorial *F*-region vertical drifts on season and solar cycle. *J. geophys. Res.* **84**, 5792.

Fejer, B. G., Paula, E. R. de, Batista, I. S., Bonelli, E. and Woodman, R. F. (1989) Equatorial *F*-region vertical plasma drifts during solar maxima. *J. geophys. Res.* **94**, 12049.

Fesen, C. G. and Abreu, V. J. (1987) Modelling the 6300-Å low-latitude nightglow. *J. geophys. Res.* **92**, 1231.

Hedin, A. E. (1983) A revised thermospheric model based on mass spectrometer and incoherent scatter data: MSIS-83. *J. geophys. Res.* **88**, 10,170.

Hedin, A. E. (1987) MSIS-86 thermospheric model. *J. geophys. Res.* **92**, 4649.

Kulkarni, P. V. and Sanders, C. L. (1964) Use of a radioactivated light source for the absolute calibration of two-colour night airglow photometer. *Planet. Space Sci.* **12**, 189.

Llewellyn, S. K. and Bent, R. B. (1973) Documentation and description of the Bent ionospheric model. Rep. AFCRK-TR-73-0657, AD 772733, Air Force Cambridge Res. Lab., Bedford, MA.

Mendillo, M. and Baumgardner, J. F. (1982) Airglow characteristics of equatorial plasma depletions. *J. geophys. Res.* **87**, 7641.

Peterson, V. L. and Van Zandt, T. E. (1969) $O(^1D)$ quenching in the ionospheric *F* region. *Planet. Space Sci.* **17**, 1725.

Rawer, K. (1981) *International Reference Ionosphere—IRI*79 (Edited by Lincoln, J. V. and Conkright, R. O.). World Data Center A, NOAA, Boulder, CO.

Sahai, Y., Bittencourt, J. A., Teixeira, N. R. and Takahashi, H. (1981a) Plasma irregularities in the tropical *F* region detected by OI 7774 Å and 6300 Å nightglow measurements. *J. geophys. Res.* **86**, 3496.

Sahai, Y., Bittencourt, J. A., Teixeira, N. R. and Takahashi, H. (1981b) Simultaneous observations of OI 7774-Å and OI 6300-Å emissions and correlative study with ionospheric parameters. *J. geophys. Res.* **86**, 3657.

Serafimov, K., Gogoshev, M. and Gogosheva, T. S. (1977) Models of the nighttime vertical distribution of the 6300 Å emission. *Geomagn. Aer.* **17**, 702.

Sobral, J. H. A., Abdu, M. A., Batista, I. S. and Zamlutti, C. J. (1981) Wave disturbances in the low latitude ionosphere and equatorial ionospheric plasma depletions. *J. geophys. Res.* **86**, 1374.

Tinsley, B. A. and Bittencourt, J. A. (1975) Determination of *F* region height and peak electron density at night using airglow emissions from atomic oxygen. *J. geophys. Res.* **80**, 2333.

Tsunoda, R. T. (1985) Control of the seasonal and longitudinal occurrence of equatorial scintillations by the longitudinal gradient in integrated *E* region Pedersen conductivity. *J. geophys. Res.* **90**, 4547.

Weber, E. J., Buchau, J., Eather, R. H., and Mende, S. B. (1978) North–South aligned equatorial airglow depletion. *J. geophys. Res.* **83**, 712.

Woodman, R. R. (1970) Vertical drift velocities and East–West electric fields at the magnetic equator. *J. geophys. Res.* **75**, 6249.

Yano, K. (1966) Nightglow photometer using filter tilting technique. *Rep. Ionosph. Space Res. Japan* **20**, 229.